Cancer Research

ERβ-Mediated Alteration of circATP2B1 and miR-204-3p Signaling Promotes Invasion of Clear Cell Renal Cell Carcinoma

Zhenwei Han[1,2], Yong Zhang[1], Yin Sun[2], Jiaqi Chen[2], Chawnshang Chang[2], Xiaolu Wang[1], and Shuyuan Yeh[2]

Abstract

Early studies have indicated that estrogen receptor beta (ERβ) can influence the progression of clear cell renal cell carcinoma (ccRCC). Here, we report the mechanistic details of ERβ-mediated progression of ccRCC. ERβ increased ccRCC cell invasion via suppression of circular RNA ATP2B1 (circATP2B1) expression by binding directly to the 5′ promoter region of its host gene ATPase plasma membrane $Ca2^{+}$ transporting 1 (ATP2B1). ERβ-suppressed circATP2B1 then led to reduced miR-204-3p, which increased fibronectin 1 (FN1) expression and enhanced ccRCC cell invasion. Targeting ERβ with shRNA suppressed ccRCC metastasis in a murine model of RCC; adding circATP2B1 shRNA partly reversed this effect. Consistent with these experimental results, ccRCC patient survival data from The Cancer Genome Atlas indicated that a patient with higher ERβ and FN1 expression had worse overall survival and a patient with higher miR-204-3p expression had significantly better overall survival. Together, these results suggest that ERβ promotes ccRCC cell invasion by altering the ERβ/circATP2B1/miR-204-3p/FN1 axis and that therapeutic targeting of this newly identified pathway may better prevent ccRCC progression.

Significance: These results identify an ERβ/circATP2B1/miR-204-3p/FN1 signaling axis in RCC, suggesting ERβ and circular RNA ATP2B1 as prognostic biomarkers for this disease. *Cancer Res; 78(10); 2550–63. ©2018 AACR.*

Introduction

Renal cell carcinoma (RCC) is the seventh most common cancer in men and the ninth most common in women worldwide, representing approximately 2% to 3% of all adult malignancies (1). Approximately 63,990 new patients with RCC were diagnosed in 2017 in the United States, with more than 14,400 deaths (2). Clear cell RCC (ccRCC) is the most common histologic subtype of RCC. Although more and more small renal masses are detected, and radical nephrectomy is considered to be the most effective way to treat ccRCC, approximately one third of patients with ccRCC will develop metastatic lesions during the course of this disease. The 5-year survival rate of advanced ccRCC is still less than 10% (3).

There are two major types of estrogen receptors, ERα and ERβ. ERα protein was undetectable in 122 RCC cases and 7 RCC cell lines that we examined. ERβ protein is positively stained in around 55% of these RCC tissues. ERβ could play differential roles in different cancers. Previously, ERβ was recognized as a prognostic factor in breast cancer (4), yet ERβ was also found to promote progression in bladder cancer (5). Furthermore, Panza and colleagues reported that ERβ can suppress seminoma through the transcriptional regulation of SIRT 3 (6). However, there are some studies suggesting a proliferative and survival role for ERβ in breast cancer (7) and prostate cancer (8). Nakajima and colleagues reported that the lower dose of E2 inhibited PDGFA transcription and suppressed angiogenesis through ERβ in prostate cancer (9). Slusarz and colleagues showed that ERα promotes and ERβ prevents/reduces the incidence of poorly differentiated prostate carcinoma (10). On the other hand, ERβ may either play a protective role during early stages of prostate carcinogenesis, yet promote metastasis during the later stages (11, 12). Also, a significant increase of ERβ expression is observed in more than half of the patients after progression to castration-resistant prostate cancer (12). Furthermore, ERβ-dependent cell proliferation through both genomic and nongenomic pathways has been shown in lung carcinoma cells (13), and in esophageal squamous cell carcinoma (14). Together, ERβ could either upregulate or downregulate its target genes at the transcriptional level to affect the progression of different types of tumors at different stages. Recent studies suggested that ERβ could promote the ccRCC progression (15), and results from The Cancer Genome Atlas (TCGA) database analyses indicate that ERβ expression is associated with the ccRCC stage, progression, and overall survival. However, the detailed mechanisms how ERβ regulates the RCC progression remain to be further elucidated.

Noncoding RNAs (ncRNA) include long noncoding RNAs (lncRNA), pseudogenes, circular RNAs (circRNA), and microRNA (miRNAs, miRs). These RNA transcripts could act like competing

[1]Department of Urology, the Second Hospital of Hebei Medical University, Shijiazhuang, China. [2]George Whipple Lab for Cancer Research, Departments of Urology, Pathology, Radiation Oncology, and The Wilmot Cancer Center, University of Rochester Medical Center, Rochester, New York.

Note: Supplementary data for this article are available at Cancer Research Online (http://cancerres.aacrjournals.org/).

Z. Han and Y. Zhang contributed equally to this article.

Corresponding Authors: Shuyuan Yeh, University of Rochester Medical Center, 601 Elmwood Avenue, Rochester, NY 14642. Phone: 585-273-2750; Fax: 585-756-4133; E-mail: Shuyuan_Yeh@URMC.Rochester.edu; and Xiaolu Wang, Department of Urology, the Second Hospital of Hebei Medical University, 215 West Heping Road, Shijiazhuang 050000, China. Phone: 86031166002106; Fax: 86031166002106; E-mail: wxl2106@126.com

doi: 10.1158/0008-5472.CAN-17-1575

endogenous RNAs (ceRNA). Among those ncRNAs, the circRNAs were first discovered in RNA virus in the 1970s (16), and for a long time they were recognized as the products of incorrect splicing of mRNAs. Recently, circRNAs were defined as a class of endogenous RNAs, which are widely expressed in human cells and play important roles in the regulation of gene expression at the posttranscriptional level (17). Some circRNAs may regulate gene expression via acting as a "sponge" of miRNAs (18), and some circRNAs can act as a miRNA "reservoir" to regulate tumor progression in breast or colorectal cancer (19, 20). Our new finding indicates that ERβ could regulate circRNA to control ccRCC progression. Furthermore, early studies indicated that a subset of miRNAs were either upregulated or downregulated in metastatic ccRCC (21), yet the functions of those RCC metastasis related miRNAs and how they interact with lncRNAs and circRNAs remain to be further elucidated.

Here, we found that ERβ could function through regulating the circRNA ATP2B1 (circATP2B1) and controlling the miR-204-3p to promote the ccRCC progression.

Materials and Methods

Cell lines

The 786-O, A498, Caki-1, and HEK-293 cells were all purchased from the ATCC, which performs its own authentication by short tandem repeat DNA profiling. All cell lines were expanded to passage 3, stored in aliquots in liquid nitrogen, and were used for fewer than 4 months after receipt or resuscitation from cryopreservation. Cells were grown under standard conditions and tested for *Mycoplasma* every 6 months using the Universal Mycoplasma Detection Kit (ATCC).

Lentiviral expression plasmids and virus production

The pLKO.1-shERβ, pWPI-ERβ, pLVTHM-shcircATP2B1, pWPI-circATP2B1, pLVTHM-miR-204-3p, pLVTHM-shFN1, psPAX2 packaging plasmid, and pMD2G envelope plasmid were transfected into HEK-293 cells using the standard $CaCl_2$ transfection method for 48 or 72 hours to get the lentivirus soup. The purified virus soup was used to transduce the RCC cell lines following methods in our previous reports (15, 22). The two published sequences, shown to promote circularization (23), were first engineered in the pBSK vector as pBSK(CircArm). Two exons of the *ATP2B1* gene were PCR amplified, and then inserted into the pBSK(CircArm) vector as the pBSK_circATP2B1. Then we subcloned the fragments including two exons of *ATP2B1* and those two arms to the lentiviral pWPI vector for expressing circATP2B1. The lentivirus soups for circATP2B1 could be collected for immediate use or frozen at −80°C for later use. To clone and PCR circRNA from the pBSK_circATP2B1, the forward primer is: AAAGTGCTGAGATTACAGGCGTGAGCCACCACCCCCGGCCCACTTTTTGTAAAGGTACGTACTAATGACTTTTTTTTTATACTTCAG, and the reverse primer is: GTAAGAAGCAAGGAAAAGAATTAGGCTCGGCACGGTAGCTCACACCTGTAATCCCAGCA.

RNA extraction and quantitative real-time PCR analysis

Total RNAs were isolated using TRIzol reagent (Invitrogen) conforming to the manufacturer's instructions and then 2 μg RNA was used for reverse transcription using Superscript III transcriptase (Invitrogen). Quantitative real-time PCR (qRT-PCR) was applied using a Bio-Rad CFX96 system with SYBR Green to determine the mRNA expression level of a gene of interest.

Cell invasion assay

Cells were seeded in 6-well plates and incubated for 72 hours after the designated treatments. The upper chambers of 8.0-μm pore size polycarbonate membrane filters (Corning Incorporated) were coated with diluted Matrigel (1:20; BD Corning) 2 to 4 hours before plating the cells. Then, the cells were collected with serum-free media and plated into the upper chambers at 1×10^5/mL, and 750 μL 10% FBS media were added into the lower chambers for incubation at 37°C in 5% (v/v) CO_2 incubator for 6 to 8 hours. The noninvading cells and Matrigel in the upper chambers were removed gently by cotton swabs, and cells invaded to the bottom of the membranes were permeabilized by methanol and stained with 0.1% (w/v) crystal violet. The invaded cells were counted in five randomly chosen microscopic fields (100×) in each experiment and averaged for quantification. Each sample was run in triplicate and in multiple experiments.

3D invasion assay

We mixed Matrigel and collagen I (1:1) and 250 μL of the mixture were evenly loaded to each well of 24-well plates (at 125 μL/cm^2). After the mixture of Matrigel and collagen I solidified, 1×10^4 ccRCC cells were mixed with solution containing 5% Matrigel and 10 ng/mL EGF and seeded in each well. The media were replenished every 3 days. After 8 to 10 days of incubation, cell structures were imaged (200×), and the numbers of protrusion structures were counted in each field. The quantification of invasion ability was measured by the number of protrusion structures of each sphere. We counted 30 spheres and the data were averaged and normalized to the vector control group. The final results are shown as a relative protrusion number count (fold).

Chromatin immunoprecipitation assay

Cells were treated with 4% formaldehyde for 10 minutes to cross-link the protein–genomic DNA complex, followed by cell collection and sonication with a predetermined power to yield genomic DNA fragments of 300 to 1,000 bp long. Lysates were preincubated with protein A-agarose conjugated normal rabbit IgG (sc-2027, Santa Cruz Biotechnology). Anti-ERβ antibody (Abcam, #N2C2, 5.0 μg) was then added to the cell lysates at 4°C for overnight. IgG was used as the negative control. Specific primer sets were designed to amplify a target sequence within human *ATP2B1* gene's promoter. PCR products were analyzed by agarose gel electrophoresis and qRT-PCR.

Luciferase reporter assays

The human 5′-promoter region of *ATP2B1* gene was constructed into pGL3-basic luciferase reporter vector (Promega). Site-directed mutagenesis of the ERβ binding site in the ATP2B1 5′ promoter was achieved with the Quick Change mutagenesis. The 1,100-bp fragment of FN1 3′ untranslated region (3′UTR) with wild-type (WT) or mutant miRNA-responsive elements was cloned into the psiCHECK2 vector (Promega) downstream of the Renilla luciferase ORF. 786-O and A498 cells were plated in 24-well plates, and the cDNA were transfected with Lipofectamine 3000 transfection reagent (Invitrogen) according to the manufacturer's instructions. PRL-TK was used as an internal control that served as the baseline control response. Luciferase activity was measured 36 to 48 hours after transfection by Dual-Luciferase Assay (Promega) according to the manufacturer's manual.

The circRNA–miRNA pulldown assay

The cells were collected in cell lysis buffer after receiving the designated treatments for 72 hours. The qRT-PCR was used to test the levels of GAPDH to ensure that the input of each group was equal for the following steps. The cell lysate mixture was rotated overnight at 4°C after adding 1.5 μL RNase inhibitor and 500 pmol/L biotin-labeled antisense oligos against circATP2B1 (5′-GGATAA TGCACATGTGTATATCT-3′). The lysate mixture was rotated for 2 hours at 4°C after adding 10 μL Streptavidin Agarose beads. The mixture was centrifuged at 3,000 rpm for 2 minutes, and then the beads were washed with cell lysis buffer 5 times. Total RNA was extracted by TRIzol (Invitrogen) according to the manufacturer's protocol, reverse transcribed, and subjected to qPCR analysis to detect the circRNA ATP2B1 miRNAs.

In vivo mouse ccRCC model

Thirty-two 6- to 8-week-old athymic NCr-nu/nu female mice were purchased from NCI and divided into 4 groups for orthotopic implantation of 1×10^6 786-O-Luc cells transduced with (i) pLKO + pLVTHM, (ii) shERβ + pLVTHM, (iii) pLKO + shcircATP2B1, or (iv) shERβ + shcircATP2B1 (mixed with Matrigel, 1:1) under the capsule of the right kidney. Tumor development and metastasis were monitored by the Fluorescent Imager (IVIS Spectrum, Caliper Life Sciences) once a week. Mice were sacrificed after 6 weeks, tumors and any metastases were then removed for further characterization. The Institutional Animal Care and Use Committee (IACUC) review board at University of Rochester has approved the studies.

Statistical analysis

All experiments were performed in triplicate per each experiment and at least 3 independent experiments. The data were presented as means ± SD. Statistical analyses involved paired *t* test with SPSS 17.0 (SPSS Inc.). $P < 0.05$ was considered statistically significant.

Results

ERβ promoted ccRCC cell invasion

Early studies indicated that ERβ may function as an oncogene to promote the ccRCC progression (15). Its potential linkage to the circRNAs function in the regulation of ccRCC progression, however, remains unclear. Here, we first knocked down ERβ by shRNA (shERβ) in ccRCC 786-O cells that have a higher endogenous ERβ expression as well as overexpressed ERβ (oeERβ) in ccRCC A498 cells that have a lower endogenous ERβ expression (Fig. 1A). Using the Matrigel-coated Transwell invasion assay, we found that knocking down ERβ in 786-O cells (786-O-shERβ) decreased cell invasion compared with the vector control (786-O-pLKO; Fig. 1B, left two panels). In contrast, overexpressing ERβ in A498 cells (A498-oeERβ) increased cell invasion compared with the vector control group (A498-pWPI; Fig. 1B, right two panels).

Importantly, using the 3D invasion assay (24, 25) to replace the Transwell invasion assay, we obtained similar results showing that knocking down ERβ in 786-O cells (786-O-shERβ) decreased cancer cell invasion (Fig. 1C, left two panels), and overexpressing ERβ in A498 cells (A498-oeERβ) increased cell invasion ability (Fig. 1C, right two panels).

Together, results from Fig. 1 demonstrated that higher ERβ expression could increase the ccRCC cell invasion.

Human clinical data showing higher ERβ expression is associated with the higher stage and poor prognosis in patients with ccRCC

Human clinical data using the TCGA database (http://cancergenome.nih.gov) with UCSC Cancer Genome Brower (http://xena.ucsc.edu/welcome-to-ucsc-xena/) revealed that patients with higher ERβ (also known as ESR2) mRNA expression had a significantly worse overall survival ($P < 0.0001$, Fig. 2A), suggesting ERβ could play a promoting role in the RCC progression. Furthermore, we also analyzed the survival of different genders, and results indicated that ERβ could promote the RCC progression in male as well as in female patients with RCC ($P = 0.0004$, Fig. 2B, and $P = 0.0348$, Fig. 2C, respectively), but the overall survival had no significant differences if compared between male and female patients with RCC ($P = 0.6236$, Fig. 2D). In addition, our analysis showed that the ERβ mRNA level was significantly higher in T3/T4 stages compared with T1/T2 stages ($P = 0.0009$, Fig. 2E).

In summary, results from TCGA human clinical sample surveys suggest that a higher ERβ expression was associated with the advanced stages and the poor prognosis in patients with ccRCC, which is in agreement with our *in vitro* data from multiple ccRCC cells showing ERβ can play a promoting role for the ccRCC progression.

ERβ enhanced ccRCC cells invasion via downregulating the circATP2B1

To dissect the molecular mechanism why ERβ can enhance ccRCC cell invasion, we focused on circRNAs because early studies suggested they may play important roles via modulating the gene expression to influence the tumor progression (17). Through a bioinformatics analysis of circ2Traits (http://gyanxet-beta.com/circdb/), we first identified 76 ccRCC-related circRNAs. Our q-PCR data showed the circRNAs, 000826, 001953, and 000983, were significantly decreased when ERβ was knocked down in 786-O cells (Fig. 3A, left). However, only the circRNA 000826 (circATP2B1) was significantly increased after overexpressing ERβ in A498 cells. Thus, circRNA 001953 and 000983 are not always robustly regulated by ERβ. Of note, the ERβ regulation of circRNA 001953 and 000983 in 786-O cells may be a cell type–specific observation, which could be further studied in the future. Together, consistent results from qRT-PCR showed the circATP2B expression was modulated by ERβ. The knockdown of ERβ could increase circATP2B1 expression in 786-O cells, and adding ERβ-cDNA could decrease circATP2B1 expression in A498 cells (Fig. 3A, right).

To further confirm the ERβ knockdown specificity and effect, we constructed the 2nd ERβ-shRNA (shERβ#2) and validated the ERβ knockdown effects in another ccRCC cell line, Caki-1. Western blot data showed that either shERβ#1 or shERβ#2 could effectively knock down ERβ in these two different RCC cell lines (Fig. 3B). Knockdown of ERβ using two independent shRNAs, #1 and #2, can upregulate the circATP2B1 in both 786-O and Caki1 cells (Supplementary Fig. S1).

We also constructed two circATP2B1 shRNAs, sh-circATP2B1#1 and circATP2B1#2, to validate the roles of circATP2B1. We then applied the rescue experiments to test whether circATP2B1 knockdown can reverse the ERβ knockdown-reduced cell invasion using the Chamber-Transwell invasion assay in ccRCC cells (pLKO + pLVTHM, shERβ + pLVTHM, pLKO + shcircATP2B1, or shERβ + shcircATP2B1). The results in 786-O cells were validated using shERβ#1 and shERβ#2 as well as sh-circATP2B1#1 and sh-circATP2B1#2 (Fig. 3C). In addition to 786-O cells, the shERβ#2 and shcircATP2B1#2 were also used to validate whether

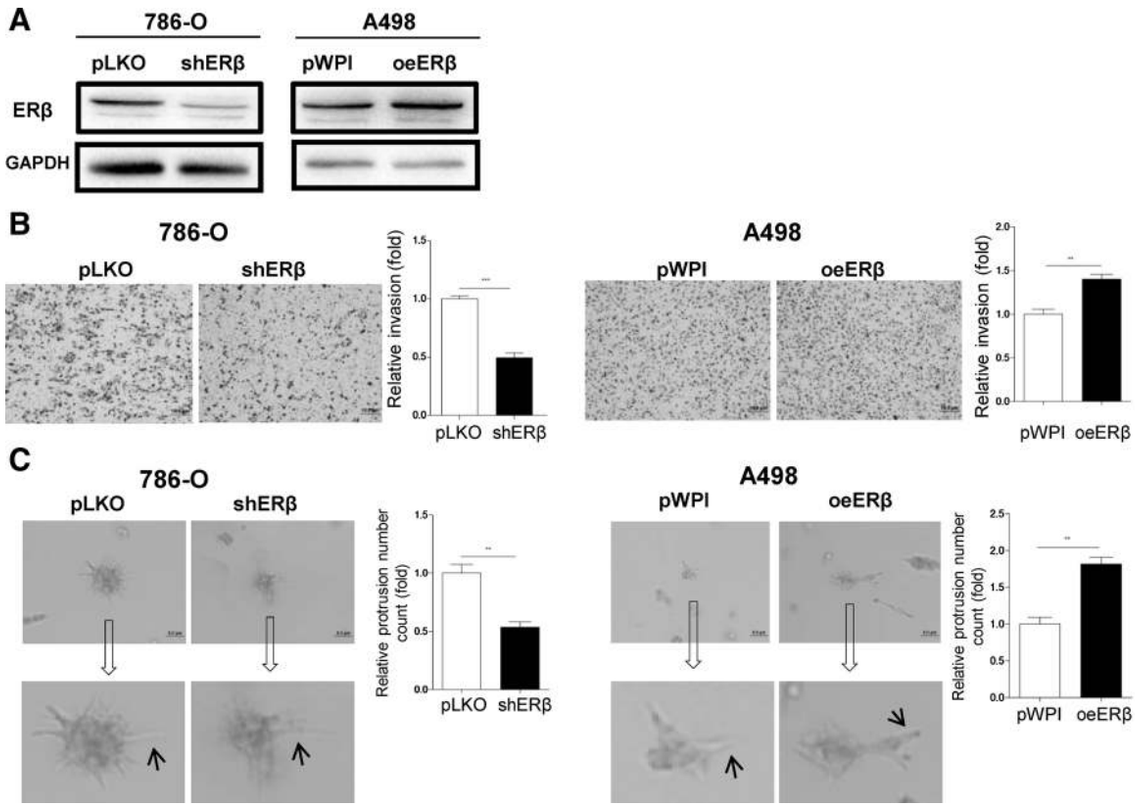

Figure 1.

ERβ promotes ccRCC cell invasion. **A,** Western blot verification of knockdown in 786-O cells (left) and ERβ overexpression in A498 cells (right). **B,** Chamber-Transwell invasion assays were performed using 786-O cells transfected with ERβ-shRNA and pLKO (left two images), and A498 cells transfected with ERβ-cDNA and pWPI (right two images) quantitations are on the right of images. The invaded cells were counted and averaged from 10 randomly chosen microscopic fields (100×). Each sample was run in triplicate and in multiple experiments. **C,** 3D invasion assays were performed in 786-O cells transduced with ERβ-shRNA and pLKO vector control (left two images), and in A498 cells transfected with ERβ-cDNA and pWPI vector (right two images), quantitations on the right of images. Sphere structures were captured in 10 different random fields under 200× microscope. Thirty spheres were counted, and the total protrusion numbers were averaged to each sphere. More protrusion structures were formed in overexpressed ERβ cells than in knocked down ERβ cells. **, $P < 0.01$; ***, $P < 0.001$ compared with the controls.

circATP2B1 knockdown can reverse the ERβ knockdown-reduced cell invasion in Caki-1 cells (Fig. 3D). In addition, we examined whether oecircATP2B1 can reverse the oeERβ-induced RCC invasion in A498 cells (Fig. 3E, pWPI + pWPI, oeERβ + pWPI, pWPI + oecircATP2B1, or oeERβ + oecircATP2B1). The results revealed that knocking-down circATP2B1 expression could reverse the ERβ-shRNA–suppressed ccRCC cell invasion in 786-O cells and in Caki-1 cells (Figs. 3C and D). Also, expression of circATP2B1 led to blocking/reversing the ERβ-promoted ccRCC cell invasion in A498 cells (Fig. 3E).

Together, Fig. 3 and Supplementary Fig. S1 results collected from different RCC cell lines, two independent ERβ shRNAs (#1 and #2) and two independent circATP2B1 shRNAs (#1 and #2) consistently suggest that ERβ could enhance RCC cell invasion via regulating circATP2B1 expression.

Mechanism dissection how ERβ regulates circATP2B1 expression

The circRNAs are produced by transcription and splicing their host gene (26). Thus, many circRNAs are proportional to their host gene expression. The circATP2B1 host gene, *ATP2B1*, was further studied to understand how ERβ regulates circATP2B1 expression (27). We applied the Ensembl and PROMO 3.0 website approaches to search for the potential estrogen response elements (ERE) on the 2-kb 5′-promoter region of *ATP2B1* and found one potential ERE within −1768nt to −1754nt (Fig. 4A). We then performed Chromatin immunoprecipitation (ChIP) binding assays in RCC cells, and found that ERβ could specifically bind to this ERE (Fig. 4B). In addition, another ERE binding site on the Hotair promoter (28) was applied as a positive control, and a region (−2268nt to −2254nt) that is around 500 bp upstream from the identified circATP2B1 ERE was applied as a negative control for the ChIP assay (Fig. 4C). We then mutated the key sequences of ERE from −1765nt to −1760nt (Fig. 4D) and applied the luciferase reporter assay in ccRCC cells. The results revealed that knocking down ERβ showed an increased luciferase reporter activity in 786-O cells with the WT ERE (Fig. 4E) and the shERβ-increased luciferase activity was abolished when ERE was mutated (Fig. 4E). We also showed that overexpression of ERβ in the A498 cells can reduce the WT ERE-luciferase reporter activity and the reduction effect is eliminated in the cells with mutant ERE-luciferase reporter (Fig. 4F).

Together, results from Fig. 4 demonstrated that ERβ could modulate circATP2B1 expression through regulating its host gene

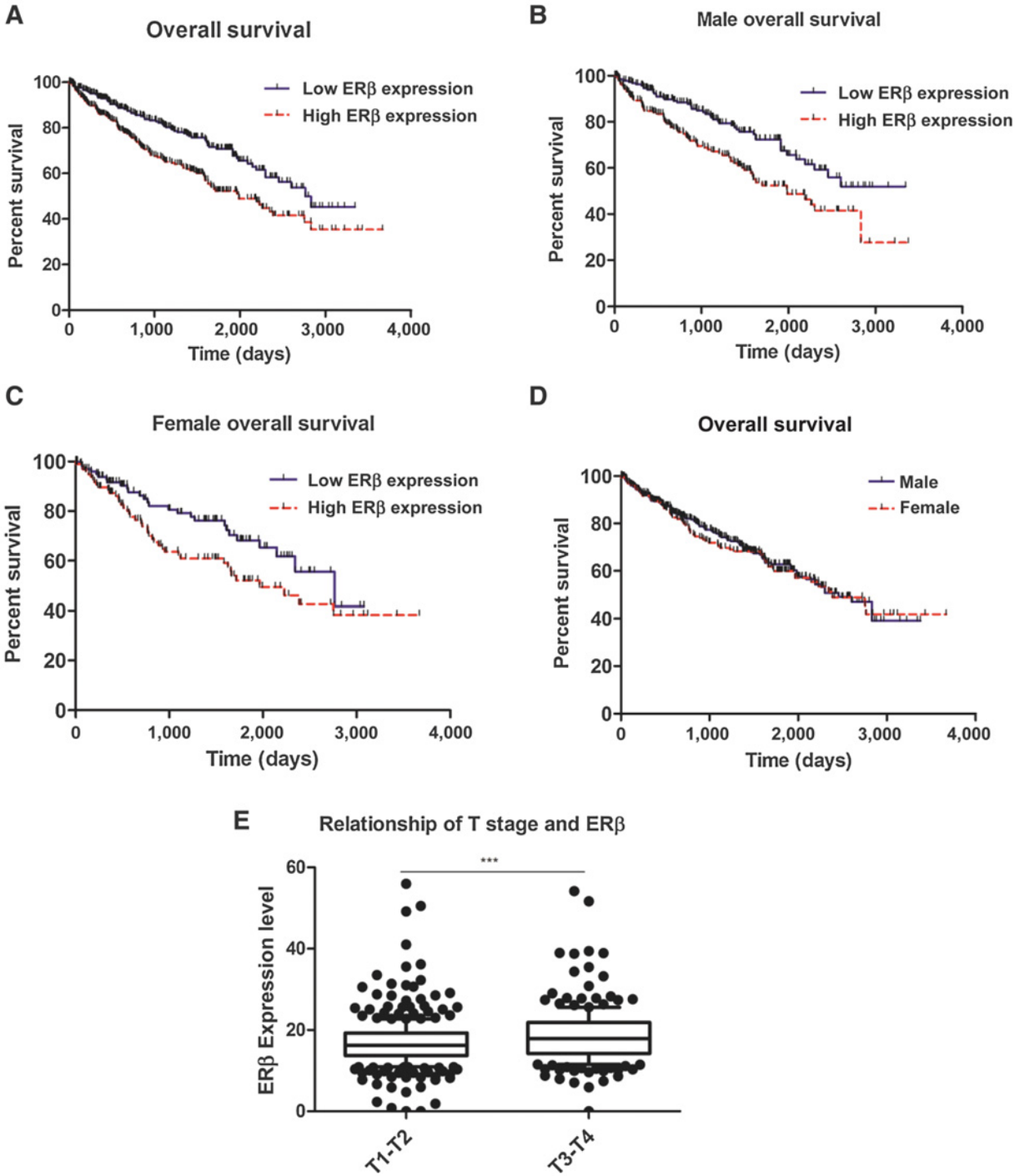

Figure 2.

Higher expression levels of ERβ were associated with higher stages and poor prognosis in patients with RCC. **A,** Overall survival curve based on TCGA database indicated that higher levels of ERβ were associated with a worse survival rate ($n = 600$; ERβ mRNA levels lower than 50% vs. higher than 50%; $P < 0.0001$). **B–C**, Overall survival curves indicated that patients with ccRCC with higher levels of ERβ were associated with shorter survival rate in male (**C**) patients, and in female (**C**) patients (male $n = 393$, $P = 0.0004$; female $n = 207$, $P = 0.0348$). **D,** Overall survival rate was similar between male and female patients with RCC ($n = 600$; $P = 0.6236$). **E,** T stage analysis based on TCGA database showed that ccRCC tissues stained with higher level of ERβ were associated with higher stage prognosis ($n = 600$; $P = 0.0009$). The T3–T4 vs. the T1–T2. ***, $P < 0.001$.

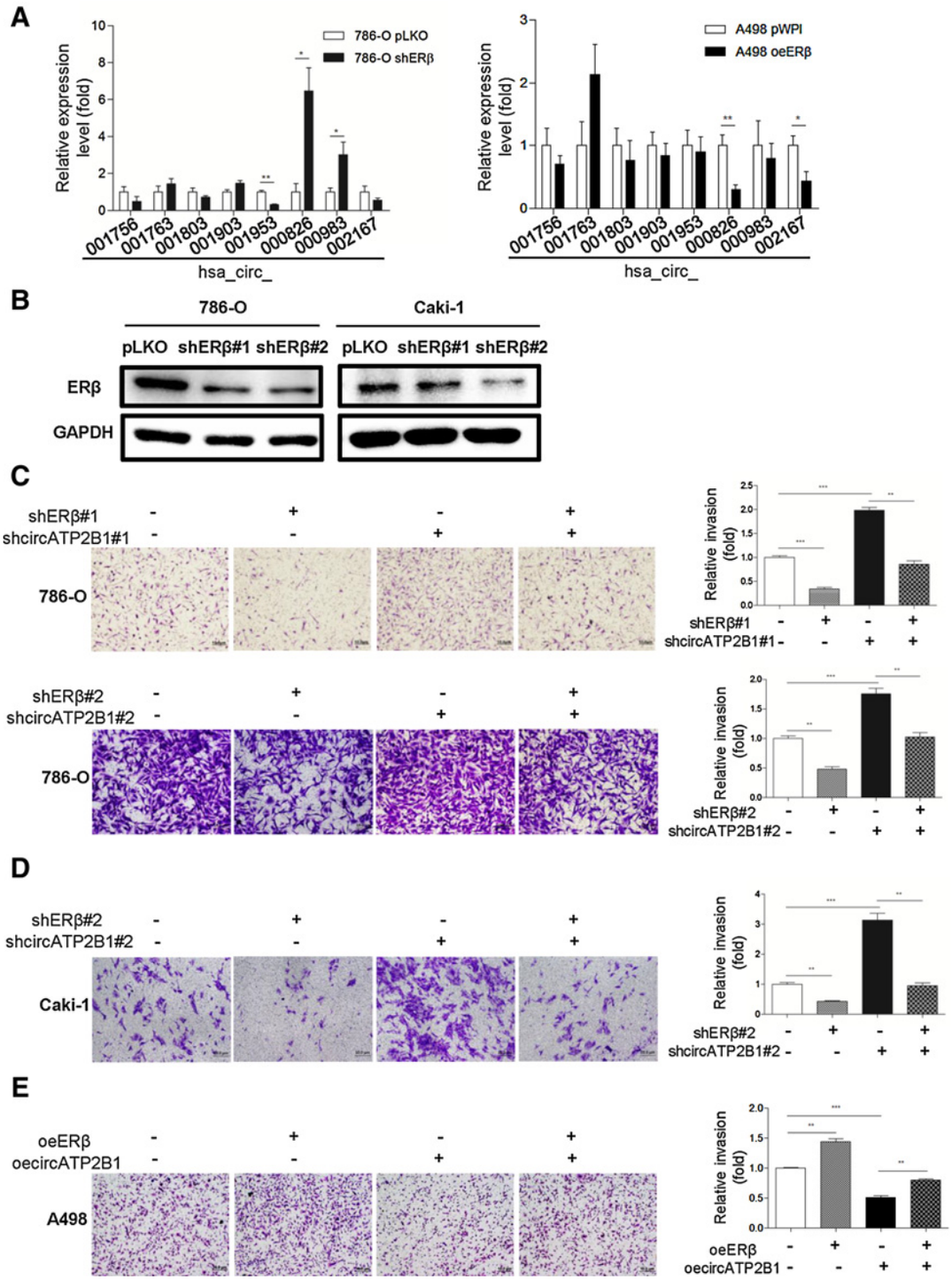

Figure 3.

ERβ enhances ccRCC cell invasion via regulating the circATP2B1 expression. **A,** Real-time PCR assay for screening a group of ccRCC-associated circRNAs in 786-O cells with knocked down ERβ (shERβ) compared with vector control (pLKO) and in A498 cells with oeERβ compared with vector (pWPI). The circATP2B1 corresponds to hsa_circ_000826. **B,** Western blot validation of ERβ knockdown by shERβ#1 and shERβ#2 in 786-O and Caki-1 cells. **C,** Chamber-Transwell invasion assays were performed using 786-O cells transfected with/without shERβ#1/shcircATP2B1#1 (top) or shERβ#2/shcircATP2B1#2 (bottom): pLKO + pLVTHM, shERβ + pLVTHM, pLKO + shcircATP2B1, or shERβ + shcircATP2B1. **D,** Chamber-Transwell invasion assays were performed using Caki-1 cells transduced with lentiviral pLKO + pLVTHM, shERβ#2 + pLVTHM, pLKO + shcircATP2B1#2, or shERβ#2 + shcircATP2B1#2. **E,** Chamber-Transwell invasion assays were performed using A498 cells transfected with/without oeERβ or circATP2B1: pWPI + pWPI, oeERβ + pWPI, pWPI + oecircATP2B1, or oeERβ + oecircATP2B1. For **C–E,** quantitations (right) are presented as relative invasion (fold); *, $P < 0.05$; **, $P < 0.01$; ***, $P < 0.001$ compared with the controls.

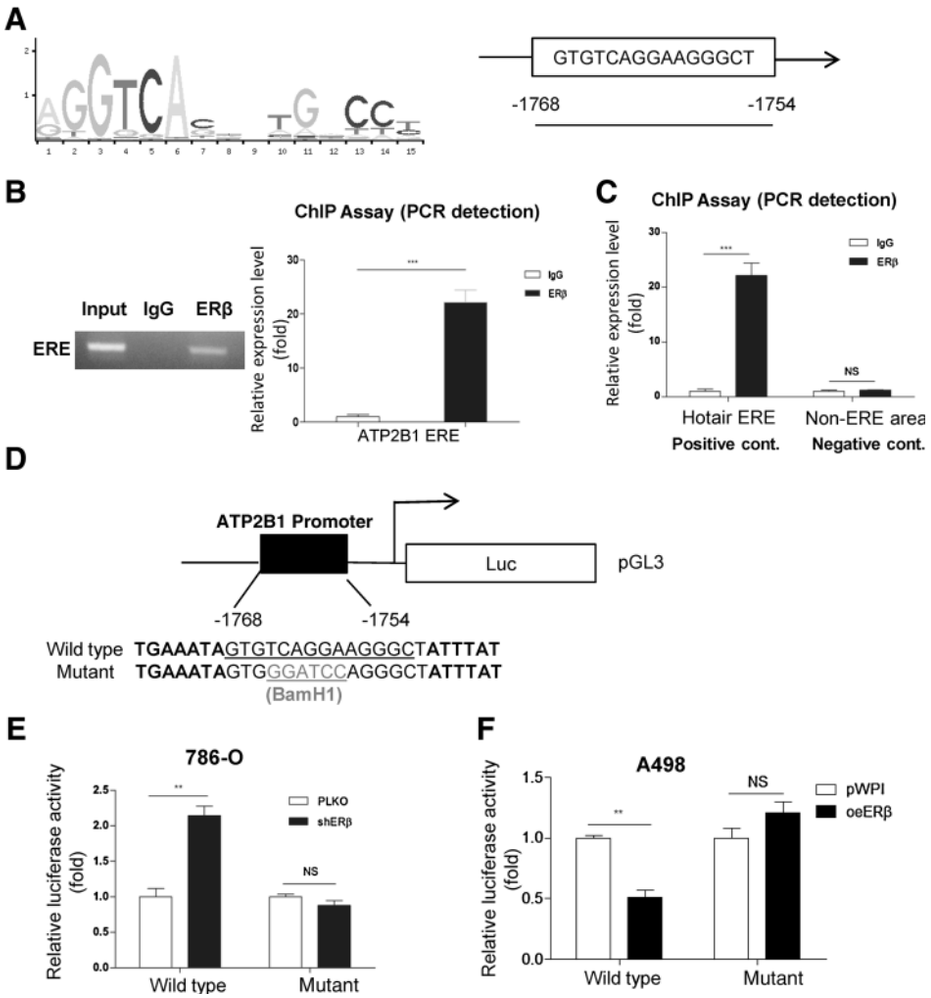

Figure 4.
Mechanism dissection of how ERβ regulates circATP2B1 expression. **A,** There is one putative estrogen response element (ERE) within the 2-Kb promoter region of ATP2B1, the host gene of circATP2B1. **B,** ChIP pulldown DNA products were amplified by PCR reaction, DNA agarose gel electrophoresis, and PCR quantified results are shown. Results revealed that the ERβ could bind to the potential ERE binding site (−1768nt to −1754nt). The IgG antibody pulldown was used as a negative control. **C,** The lncRNA Hotair promoter ERE was used as the positive control, and a promoter region (−2268nt to −2254nt) around 500 bp upstream from the identified ATP2B1 ERE site was applied as a negative control for ChIP assay. **D,** Diagram of cloning the 2-kb ATP2B1 promoter into pGL3 basic luciferase report vector (pGL3). Site-directed mutagenesis of ERE was done by mutating part of the ERE sequence into BamH1 cutting site (–GGATCC–). **E–F,** Cotransfection of ERE WT or mutant ATP2B1 promoter pGL3-Luciferase constructs into 786-O with/without shERβ (**E**) and into A498 cells with/without oeERβ (**F**). The luciferase assay was applied to detect the promoter activity. **, $P < 0.01$; NS, not significant compared with the controls.

ATP2B1 via direct binding to the ERE (−1765nt to −1760nt) on the 5′-promoter of ATP2B1.

ERβ enhanced ccRCC cell invasion via altering the circATP2B1/miR-204-3p axis

Next, to dissect the mechanism how ERβ-modulated circATP2B1 can increase the ccRCC cell invasion, we focused on the miRNAs, because circRNAs may sequester miRNAs to regulate their target genes (18). Those shERβs and shcircATP2B1s are equally effective on regulation of downstream signal expression and RCC invasion. With no special notification, there were only shERβ#1 and shcircATP2B1#1 used in most of the following experiments.

Using two public bioinformatic prediction databases, CircNet and StarBase v2.0, we identified potential tumor suppressor miRNAs (miR-204-3p, miR-3144-3p, and miR-656-3p) that may be able to interact with circATP2B1 in ccRCC. We first found that knocking down circATP2B1 in A498 cells decreased the expression of miR-204-3p and miR-3144-3p, while adding circATP2B1 in 786-O cells could only significantly increase the expression of miR-204-3p among those 3 miRNA candidates (Fig. 5A). We further applied RNA pulldown assay to test whether circATP2B1 could interact with those candidate miRNAs using the biotinylated oligonucleotides (5′-GGATAATGCACATGTGTATATCT-3′) to target the circular junction of circATP2B1. Results revealed that only miR-204-3p, but not the other two miRNAs, was enriched in the pulldown product and can directly interact with circATP2B1 (Fig. 5B). Thus, we focused on studying the circATP2B1 and miR-204-3p functional pathway.

We next applied an interruption approach to test whether changing the circRNA could influence the functional connection from ERβ to miR-204-3p expression. Results revealed that ERβ-shRNA-increased miR-204-3p could be blocked/reversed by knocking down circATP2B1 in 786-O cells (Fig. 5C). Adding circATP2B1 also reversed the ERβ-suppressed miR-204-3p expression in A498 cells (Fig. 5D), suggesting a possibility that circATP2B1 may act as a "reservoir" to stabilize the expression of the miRNA (19). To test the possibility, we compared whether the stability of miR-204-3p could be influenced by ERβ and circATP2B1 by adding actinomycin D to stop new RNA synthesis, and then determined the miRNA degradation rate at different time points by qPCR. When ERβ expression was knocked down, the knockdown of circATP2B1 could then lead to a significant reduction of remaining miR-204-3p levels while treating RCC cells with actinomycin D (Fig. 5E). Next, using the miR-204-3p inhibitor, results from the rescue approaches using Transwell invasion

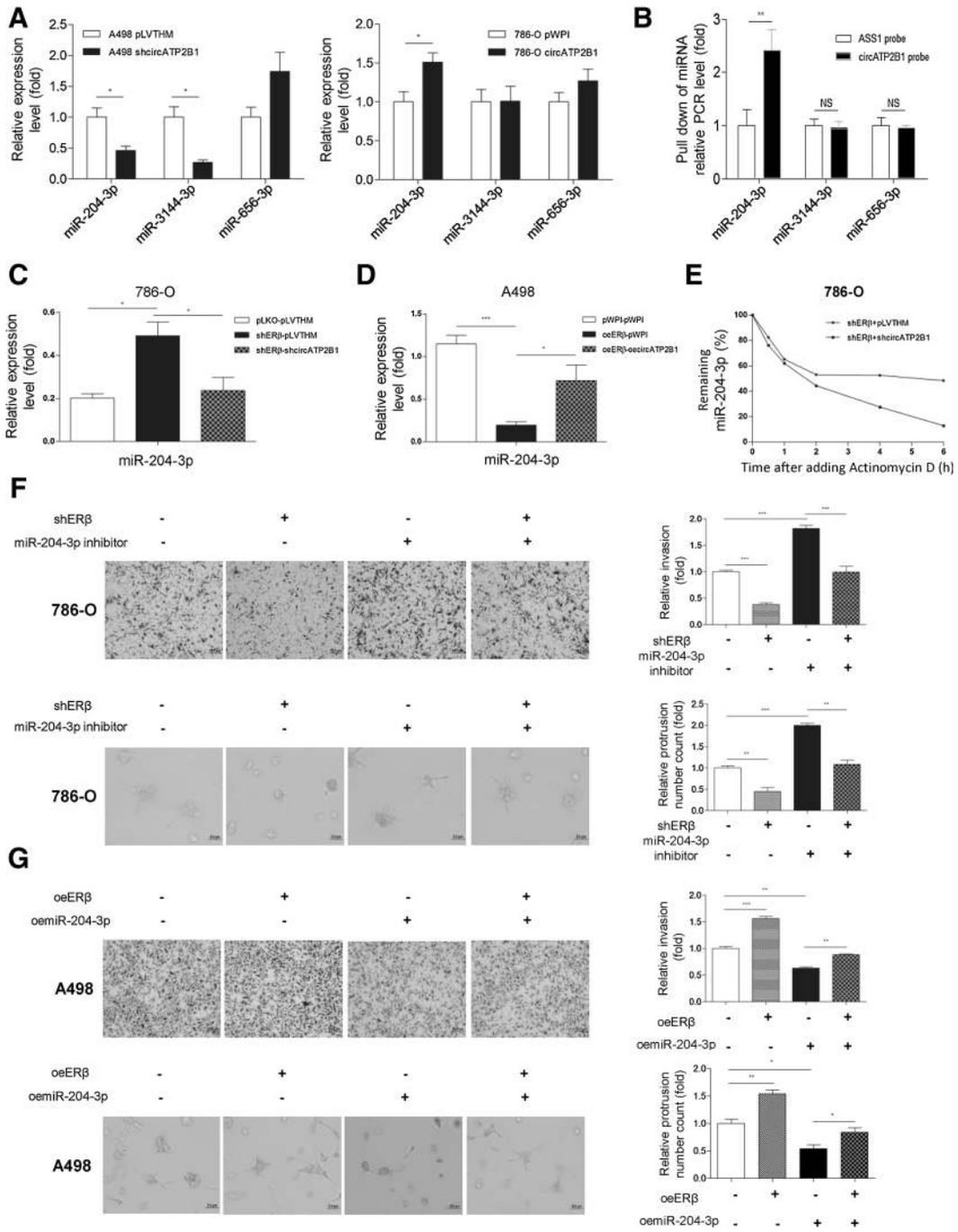

Figure 5.

ERβ enhances RCC cell invasion via altering the circATP2B1/miR-204-3p. **A,** The qRT-PCR assay for screening some circATP2B1-associated miRNAs in A498 cells with knockdown of circATP2B1 compared with vector control (shcircATP2B1#1 vs. pLVTHM; left) and in 786-O cells with overexpression of circATP2B1 compared with vector (oe circATP2B1 vs. pWPI; right). **B,** RNA pulldown assays were performed by biotinylated antisense oligo specific for the circular junction of circATP2B1. The oligo specific for the ASS1 probe was used as negative control. The miR-204-3p was enriched in biotinylated circATP2B1 oligo pulldown product, but miR-3144-3p and miR-656-3p were not detectable. **C,** Rescue assay using 786-O cells transduced with sh-circATP2B1 showed a reversed ERβ knockdown–increased miR-204-3p level. **D,** Rescue assay using A498 cells with oecircATP2B1 showed partial reversal of the ERβ-reduced miR-204-3p level. **E,** The circATP2B1 influences the miRNA204-3p stability. The 786-O cells were transduced with shERβ#1 + pLVTHM or shERβ#1 + shcircATP2B1 lentiviruses. After 72 hours, cells were exposed to actinomycin D for 0, 0.5, 1, 2, 4, and 6 hours. Then, cells were harvested for qRT-PCR to test the stability of miR-204-3p. **F,** Chamber-Transwell invasion (top) assay and 3D invasion (bottom) assay were performed using 786-O cells transfected with pLKO + Ctl, shERβ#1 + Ctl, pLKO + miR-204-3p inhibitor, or shERβ#1 + miR-204-3p inhibitor. **G,** Chamber-Transwell invasion (top) and 3D invasion (bottom) assays were performed using A498 cells transfected with pWPI + pLVTHM, oeERβ + pLVTHM, pWPI + oemiR-204-3p, or oeERβ + oemiR-204-3p. In **F–G**, the quantitations are shown on the right and are presented as a relative change (fold); *, $P < 0.05$; **, $P < 0.01$; ***, $P < 0.001$; NS, not significant compared with the controls. As shERβs and shcircATP2B1s are equally effective on regulation of downstream signal expression and RCC invasion; shERβ#1 and shcircATP2B1#1 was used in most of Fig. 5 and 6 experiments.

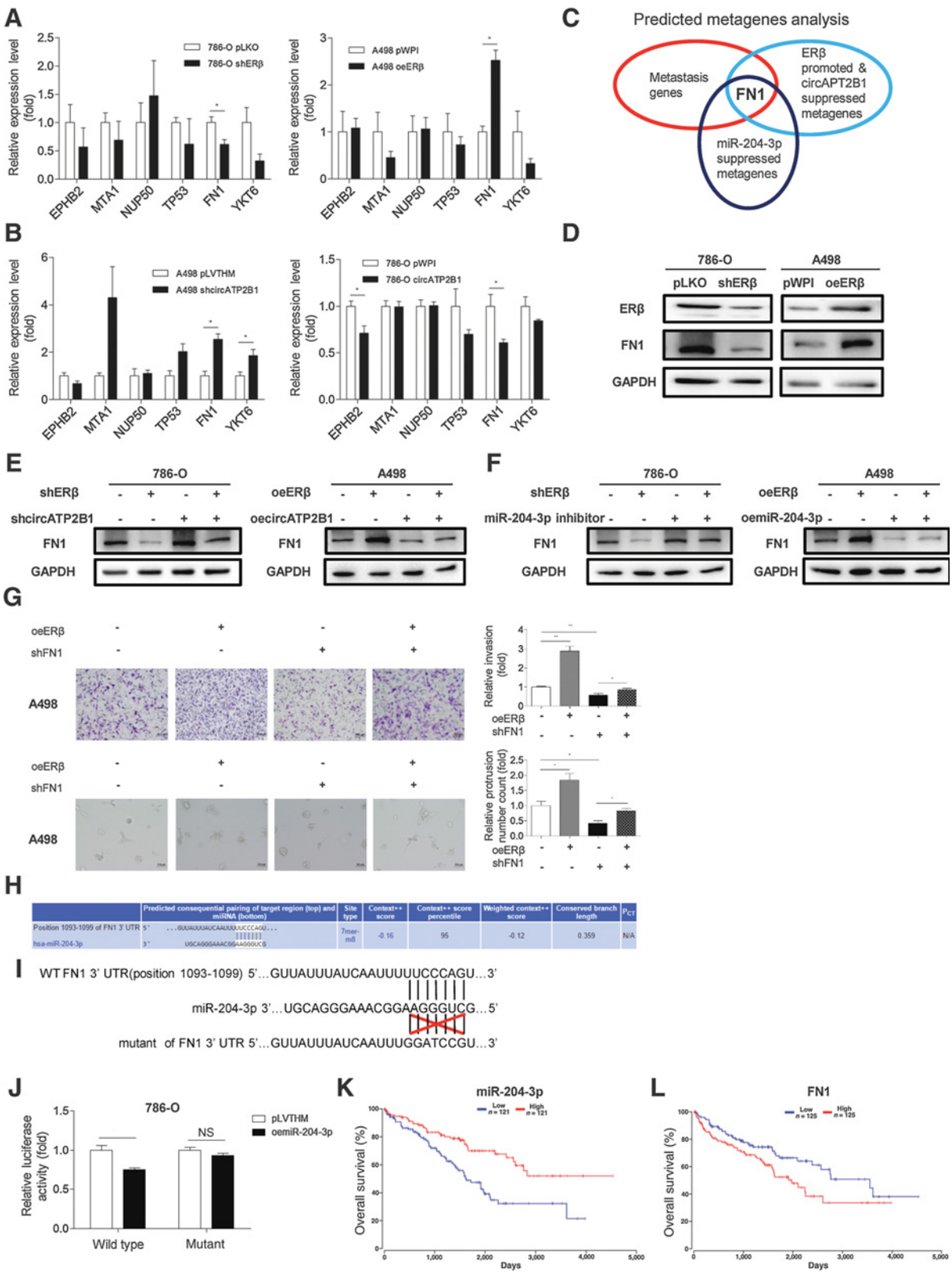

(top) assay and 3D invasion (bottom) assay revealed that an miR-204-3p inhibitor could reverse the ERβshRNA-reduced ccRCC invasion in 786-O cells (Fig. 5F). In contrast, adding miR-204-3p could block the oeERb-increased ERβ-increased ccRCC invasion in A498 cells (Fig. 5G). The above 3D invasion related data were also characterized and summarized in Supplementary Fig. S2.

Together, results from Fig. 5 and Supplementary Fig. S2 suggest ERβ-circATP2B1 may function through interacting with and modulating miR-204-3p expression to alter ccRCC cell invasion.

ERβ/circATP2B1/miR204-3p axis promoted ccRCC cell invasion via altering FN1 expression

To further dissect how the ERβ/circATP2B1/miR-204-3p axis can enhance ccRCC cell invasion, we searched for those metastasis genes that are linked to the ERβ, circATP2B1, or miR-204-3p in the ccRCC cell databases (circBase, CircNet, and OncoLnc). We focused on six metastasis-related genes, *EPHB2*, *MTA1*, *NUp50*, *FN1*, and *YKT6*, to further test their expressions with qRT-PCR. Comparing the differential expressions of the genes in the two cell lines, the results revealed that FN1 had the most differential change with shERβ in 786-O cells decreasing the expression of FN1, and oeERβ in A498 cells increasing the expression of FN1 (Fig. 6A). We also screened those genes in 786-O cells with overexpressed circATP2B1 and in A498 cells with knocked down circATP2B1. The results revealed that knocking down circATP2B1 in A498 cells significantly increased the FN1 and YKT6 and overexpressing circATP2B1 in 786-O cells significantly decreased the expression of FN1 and EPHB2 (Fig. 6B). As FN1 expression showed consistent and significant changes, we decided to focus on the FN1 to further study its linkage to the ERβ, circATP2B1, and miR-204-3p (Fig. 6C).

FN1 is highly expressed in vascular endothelial cells, vascular smooth muscle, and the perivascular matrix of tumors, which would promote angiogenesis and endothelial cell migration (29, 30). Many studies found that FN1 could increase ccRCC invasion and metastasis (31, 32). We first confirmed that knocking down ERβ decreased the FN1 protein expression in 786-O cells and adding ERβ in A498 cells increased the FN1 protein expression (Fig. 6D). Then we used the shERβ RNAs to detect the ERβ knockdown-mediated downregulation of FN1 mRNA levels via qRT-PCR in 786-O cells and Caki-1 cells, and consistent results were obtained when two independent shERβ constructs were tested (Supplementary Fig. S1). We then confirmed that knocking down circATP2B1 increased the FN1 protein expression and could partly reverse the ERβ-shRNA–suppressed FN1 expression in 786-O cells, whereas in A498 cells, adding circATP2B1 decreased the FN1 protein expression and could effectively reverse the ERβ-increased FN1 expression (Fig. 6E).

Importantly, we found that treating 786-O cells with a miR-204-3p inhibitor increased the FN1 expression and partly reversed the ERβ-shRNA–suppressed FN1 expression, while in A498 cells adding miR-204-3p decreased the FN1 expression and effectively reversed the ERβ-increased FN1 expression (Fig. 6F). Next, to examine the consequences after suppressing the FN1 expression in ccRCC cells, we applied the interruption approach using FN1-shRNA. The rescue experiments via Chamber-Transwell invasion (top) assay and 3D invasion (bottom) assay results revealed that FN1 knockdown by shRNA could effectively reduce the ERβ-enhanced ccRCC cell invasion in A498 cells (Fig. 6G). The above 3D invasion related data were also characterized and summarized in Supplementary Fig. S2.

For mechanism dissection of how miR-204-3p can modulate FN1 expression at the molecular level, we identified the potential binding site located on the 3′UTR of FN1-mRNA (http://www.targetscan.org/vert_71/; Fig. 6H). We then applied the reporter assay with the psiCHECK2 vector carrying the WT and mutant miRNA-target sites (Fig. 6I), and results revealed that miR-204-3p could decrease the luciferase reporter activity of WT 3′UTR of FN1, with little effect on the mutant 3′UTR of FN1-mRNA in 786-O cells (Fig. 6J), suggesting that miR-204-3p could directly target the 3′UTR of FN1-mRNA to suppress its protein expression.

Based on TCGA database, the data from Oncolnc (http://www.oncolnc.org/) human clinical sample surveys also showed that the patients with higher miR-204-3p expression had significantly better overall survival ($P = 0.00027$, Fig. 6K), and the patients with higher FN1 expression had poor overall survival ($P = 0.0244$, Fig. 6L).

Together, results from Fig. 6; Supplementary Figs. S1 and S2 suggest that the ERβ/circATP2B1/miR204-3p axis enhanced ccRCC cell invasion via altering the FN1 expression.

Preclinical study using *in vivo* mouse studies confirmed that ERβ promotes the ccRCC metastasis via altering the circATP2B1 expression

To further confirm all above *in vitro* cell lines data *in vivo*, we applied the preclinical study using the *in vivo* mouse RCC model with orthotopically xenografted 786-O cells expressing firefly luciferase. Female nude mice were randomly assigned into

Figure 6.

ERβ-circATP2B1-miR204-3p promotes ccRCC invasion via altering FN1 signal. **A,** The qRT-PCR assay for screening ccRCC metastasis-associated genes in 786-O cells with shERβ compared with vector pLKO (left) and in A498 cells with oeERβ compared with pWPI (right). **B,** The qRT-PCR assay for screening ccRCC metastasis–associated genes in A498 cells with knocked down circATP2B1 compared with pLVTHM vector (left) and in 786-O cells with overexpressed circATP2B1 compared with pWPI vector (right). **C,** Diagram showing that FN1 may be the ccRCC metastasis-related gene regulated by ERβ, circATP2B1, and miR-204-3p in ccRCC cells. **D,** ERβ could upregulate FN1 in ccRCC 786-O and A498 cells. Western blot assay for FN1 expression in 786-O cells with knocked down ERβ or control (left) and in A498 cells with overexpressed ERβ or control (right). **E,** Western blot assays were performed on 786-O cells transfected with pLKO + pLVTHM, shERβ#1 + pLVTHM, pLKO + shcircATP2B1#1, or shERβ#1 + shcircATP2B1#1 (left) and on A498 cells transfected with pWPI + pWPI, oeERβ + pWPI, pWPI + oecircATP2B1, or oeERβ + oecircATP2B1 (right). **F,** Western blot assay was performed on 786-O cells transfected with pLKO + Ctrl, shERβ#1 + Ctrl, pLKO + miR-204-3p inhibitor, or shERβ#1 + miR-204-3p inhibitor (left) and on A498 cells transfected with pWPI + pLVTHM, oeERβ + pLVTHM, pWPI + oemiR-204-3p, or oeERβ + oemiR-204-3p (right). **G,** Chamber-Transwell invasion assay (top) and 3D invasion assay (bottom) were performed using 786-O cells transfected with pWPI + pLVTHM, oeERβ + pLVTHM, pWPI + shFN1, or oeERβ + shFN1. **H–I**, Predicted sequence alignment of FN1 3′ UTR with WT versus mutant potential miR-204-3p targeting site. **J,** Luciferase assay was performed in 786-O cells transduced with pGL3-FN1_WT3′UTR + pLVTHM, pGL3-FN1_mut3′UTR + pLVTHM, pGL3-FN1_WT 3′UTR + miR-204-3p, or pGL3-FN1_mut 3′UTR + miR-204-3p. **K,** Survival curve from Oncolnc indicated that patients with ccRCC with higher miR-204-3p expression had significantly better overall survival ($n = 506$; patients with ccRCC with the lowest 25% miR-204-3p expression vs. the highest 25% expression; $P = 0.00027$). **L,** The patients with ccRCC with higher FN1 expression had poor overall survival ($n = 522$; the lowest 25% vs. the highest 25%; $P = 0.0244$). All quantitations are presented as means ± SD; *, $P < 0.05$; **, $P < 0.01$; ***, $P < 0.001$ compared with the controls.

4 groups with 8 mice/group and 1×10^6 786-O-Luc cells transduced with (i) pLKO + pLVTHM, (ii) shERβ + pLVTHM, (iii) pLKO + shcircATP2B1, or (iv) shERβ + shcircATP2B1 were implanted into the right subrenal capsule of female mice, and metastatic tumors were evaluated weekly using an *in vivo* imaging system (IVIS). After 6 weeks, we found an increase of metastatic luciferase signal in the shcircATP2B1 groups (Fig. 7A). Then, we sacrificed the mice and counted the number of metastatic foci in liver, intestine, spleen, and left kidney with IVIS detection (Fig. 7B–E, respectively). The results revealed that suppressing ERβ with shERβ led to a decrease of total metastatic foci, and targeting the circATP2B1 with shcircATP2B1 could partly reverse the ERβ-shRNA–suppressed ccRCC metastasis (Fig. 7F and G). Importantly, results from IHC staining demonstrated that knocking-down ERβ led to a decreased FN1 expression, which could be partly reversed after knocking-down circATP2B1 (Fig. 7H). The IHC data were quantified with German immunoreactive scoring method (33).

Together, results from our preclinical study using the *in vivo* mouse model in Fig. 7A–H prove that ERβ may play a promoting role for the ccRCC metastasis via modulation of the circATP2B1-regulated miR-204-3p/FN1 pathway axis.

Discussion

ERβ has been found to play important roles in progression of many hormone-related cancers, including breast, prostate, bladder, ccRCC, etc. Interestingly, results from these studies with these various tumors indicated that ERβ may play differential roles in the different types of tumors. For example, it has been demonstrated that ERβ can suppress tumor invasion and proliferation in breast cancer (4) and prostate cancer (34), while it can also promote tumor invasion and proliferation in bladder cancer (5). Yu and colleagues reported that ERβ acted as a tumor suppressor in ccRCC (35). However, more and more studies demonstrated that ERβ could be an oncogene in ccRCC (15, 22). Importantly, clinical data from the TCGA database confirm that higher ERβ expression is associated with shorter overall survival and higher T stages in patients with ccRCC, which is a powerful clinical evidence to prove ERβ may play a positive role in ccRCC progression. Also, ERβ could either upregulate or downregulate its target genes at the transcriptional level to affect the tumor progression at different stages. Our studies using multiple approaches via both *in vitro* and *in vivo* studies confirmed these key clinical data showing ERβ could significantly promote ccRCC cell invasion.

The circRNAs are widely expressed in human cells, and their expression levels are much higher than their linear isomers (36). The circRNAs have some important properties, including highly conserved sequences and a high degree of stability, as well as tissue- and stage-specific expression in mammalian cells, which allows the circRNAs to have the potential of becoming ideal biomarkers for the diagnosis of cancers (17, 18). A growing body of studies shows that there are some types of functional interplays among circRNAs, miRNAs on the regulation of gene expressions. Xie and colleagues found circ_001569 could target miR-145 in the proliferation and invasion of colorectal cancer (37). Li and colleagues found the circRNA, ITCH, could regulate the Wnt/β-catenin pathway to inhibit ESCC development (38). Wang and colleagues reported that AR could suppress circHIAT1 expression to promote ccRCC development (39). However, the functional interactions between circRNAs and miRNAs on the progression of ccRCC are still not well understood.

In our study, we identified ERβ could promote ccRCC invasion through binding to the promoter and downregulating circATP2B1. Previous studies identified that one function of circRNAs is the ability to serve as a sponge of miRNAs, which means circRNAs may play a role as miRNA inhibitors (17, 18, 37). However, circRNAs may also act in a different way to regulate miRNAs' availability and function. In our study, we found that circATP2B1 could increase miR-204-3p stability by acting as a miRNA "reservoir" to partially reverse ERβ-enhanced ccRCC invasion. The term "reservoir" should not be thought of as sequestration, as sequestration means taking the miRNAs away from their targets. Reservoir also does not mean "presentation" as there are no reports saying that circRNA will deliver a miRNA to a target through a mechanism of "trimolecular" or "multimolecular" complex interaction. Reservoir can simply mean if more circRNA is expressed, there will be more miRNA(s) binding to the circRNA, and consequently increasing the availability of miRNA(s) for binding and inhibiting their target mRNAs. Mechanism studies reveal that ERβ can promote ccRCC invasion via altering the circATP2B1/miR-204-3p signaling pathway. Whether ERβ can regulate other signals in ccRCC metastasis remains to be investigated.

The miR-204-3p has been found to be deregulated in several tumors, such as hepatocellular carcinoma, glioma, and breast cancer (40–42), and is closely related with ccRCC and upper tract urothelial carcinomas (43). In our study, we found that circATP2B1 functions as the reservoir of miR-204-3p, by stabilizing or promoting the transcription of miR-204-3p to inhibit ccRCC invasion.

FN1 is highly expressed in vascular endothelial cells, vascular smooth muscle, and the perivascular matrix of tumors, which would promote angiogenesis and endothelial cell migration (29, 30). FN1 has been proven to potentially promote progression of some kinds of tumors (44–47). In addition, some studies found that FN1 could play very important roles in promoting ccRCC invasion and metastasis (31, 32). FN1 is one of the potential target genes of miR-204-3p and has been verified by target gene prediction software, and Cui and colleagues found miR-204-3p could target FN1 in HCC (40). It has been reported that functionally the sponge and reservoir effects of circRNAs are opposite in that the sponge-type circRNAs may take away miRNAs from their targets while the reservoir-type circRNAs may help to maintain the miRNA levels and allow them to modulate their targets. There are several possibilities underlying these differences: one could be the miRNA–circRNA binding affinity and another could be the involvement of additional proteins (39, 48). In that sense, the function as "sponge" and "reservoir" of circRNA may not be mutually exclusive. When we performed the RNA pulldown experiment to detect the interaction between circATP2B1 and miRNA-204-3p (Fig. 5B), we could not detect the 3′UTR of FN1 in the pulldown complex. Thus, it is proposed that miR-204-3p will interact with circRNACTP2B1 or with the 3′UTR of FN1 on a dynamic (on–off) fashion. This dynamic (on–off) interaction fashion has also been reported with other miRNAs (49, 50). In this study, we confirmed miR-204-3p could directly target the 3′-UTR of FN1 to suppress ccRCC cell invasion.

In summary, ERβ could promote ccRCC invasion via altering the circATP2B1/miR-204-3p/FN1 signals, and targeting these

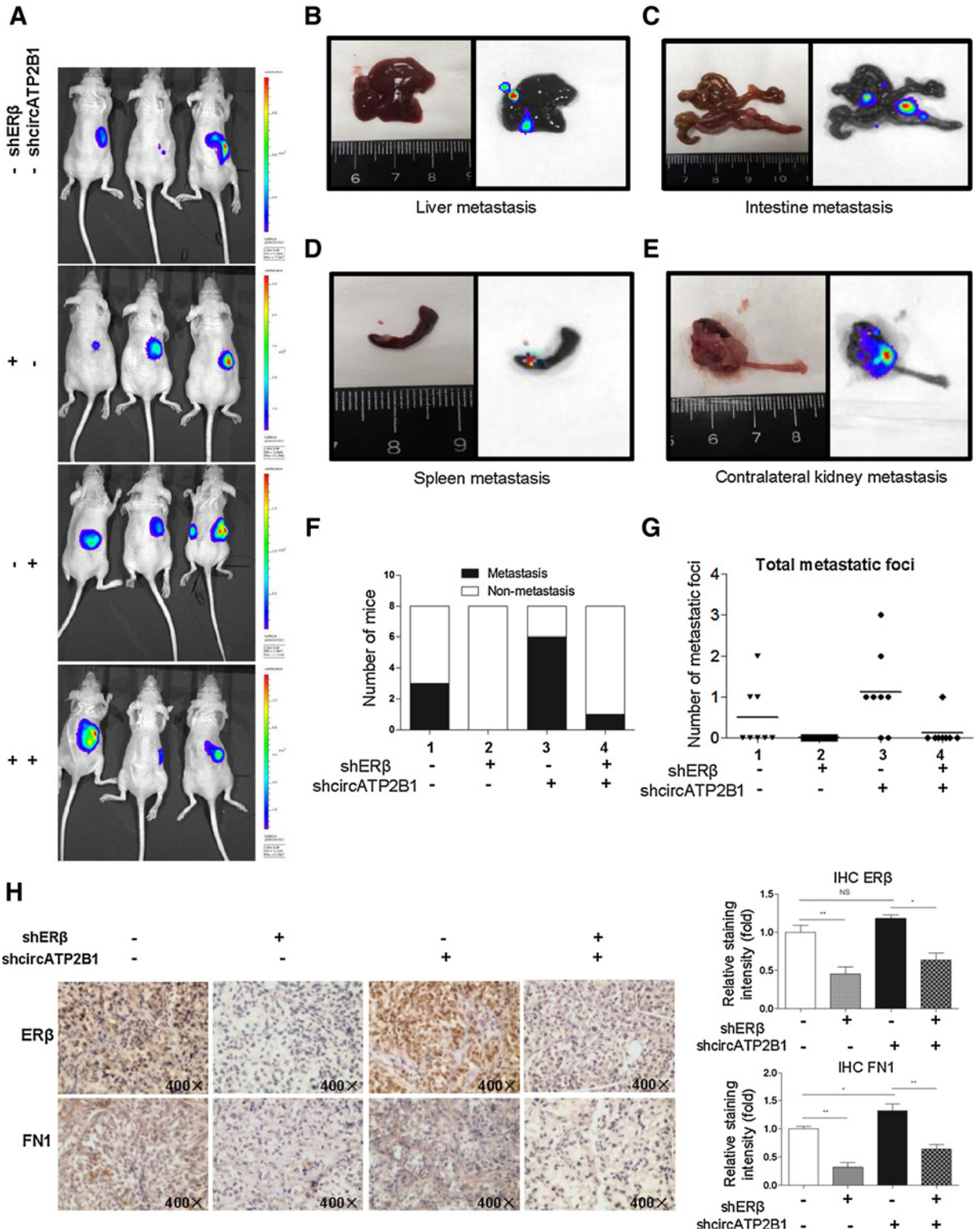

Figure 7.

In vivo mouse studies confirmed that ERβ promotes the metastasis of ccRCC via regulating circATP2B1. **A,** IVIS imaging was used to detect the various distal metastasis foci in mice with orthotopically xenografted ccRCC cells under the renal capsule of the right kidney. Three representative mouse IVIS bioluminescent images are shown. **B–E,** Representative organ bioluminescent images showing metastasis from liver, intestine, spleen, and the left kidney. **F,** Quantification of the metastases in the mice. **G,** Quantification of the total metastatic foci. **H,** Representative images of IHC staining for ERβ and FN1. Right, quantitations. *, $P < 0.05$; **, $P < 0.01$ compared with the controls.

newly identified signals may help us to develop a new therapy to better suppress the ccRCC progression.

Disclosure of Potential Conflicts of Interest

No potential conflicts of interest were disclosed.

Authors' Contributions

Conception and design: S. Yeh
Development of methodology: Y. Zhang, Y. Sun, S. Yeh
Acquisition of data (provided animals, acquired and managed patients, provided facilities, etc.): Z. Han, J. Chen
Analysis and interpretation of data (e.g., statistical analysis, biostatistics, computational analysis): Z. Han, Y. Zhang, C. Chang
Writing, review, and/or revision of the manuscript: Z. Han, C. Chang, S. Yeh
Administrative, technical, or material support (i.e., reporting or organizing data, constructing databases): Y. Sun, X. Wang
Study supervision: X. Wang, S. Yeh

Acknowledgments

This work was supported by the URMC Urology research fund (S. Yeh) and the George Whipple Professorship Endowment (C. Chang). We thank Ms. Karen Wolf for helping with the preparation of the manuscript.

The costs of publication of this article were defrayed in part by the payment of page charges. This article must therefore be hereby marked *advertisement* in accordance with 18 U.S.C. Section 1734 solely to indicate this fact.

Received June 3, 2017; revised December 14, 2017; accepted February 23, 2018; published first February 28, 2018.

References

1. Rini BI, Campbell SC, Escudier B. Renal cell carcinoma. Lancet 2009; 373:1119–32.
2. Rebecca L SM, Kimberly D, Miller MPH, Ahmedin Jemal DVM. Cancer statistics, 2017. CA: Cancer J Clin 2017;67:7–30.
3. Stadler WM. Targeted agents for the treatment of advanced renal cell carcinoma. Cancer 2005;104:2323–33.
4. Paruthiyil S, Parmar H, Kerekatte V, Cunha GR, Firestone GL, Leitman DC. Estrogen receptor beta inhibits human breast cancer cell proliferation and tumor formation by causing a G2 cell cycle arrest. Cancer Res 2004;64:423–8.
5. Hsu I, Chuang KL, Slavin S, Da J, Lim WX, Pang ST, et al. Suppression of ERbeta signaling via ERbeta knockout or antagonist protects against bladder cancer development. Carcinogenesis 2014;35:651–61.
6. Panza S, Santoro M, De Amicis F, Morelli C, Passarelli V, D'Aquila P, et al. Estradiol via estrogen receptor beta influences ROS levels through the transcriptional regulation of SIRT3 in human seminoma TCam-2 cells. Tumour Biol 2017;39:1010428317701642.
7. Leygue E, Murphy LC. A bi-faceted role of estrogen receptor beta in breast cancer. Endocr Relat Cancer 2013;20:R127–39.
8. Nelson AW, Tilley WD, Neal DE, Carroll JS. Estrogen receptor beta in prostate cancer: friend or foe? Endocr Relat Cancer 2014;21:T219–34.
9. Nakajima Y, Osakabe A, Waku T, Suzuki T, Akaogi K, Fujimura T, et al. Estrogen exhibits a biphasic effect on prostate tumor growth through the estrogen receptor beta-KLF5 pathway. Mol Cell Biol 2016;36:144–56.
10. Slusarz A, Jackson GA, Day JK, Shenouda NS, Bogener JL, Browning JD, et al. Aggressive prostate cancer is prevented in ERalphaKO mice and stimulated in ERbetaKO TRAMP mice. Endocrinology 2012;153: 4160–70.
11. Fixemer T, Remberger K, Bonkhoff H. Differential expression of the estrogen receptor beta (ERbeta) in human prostate tissue, premalignant changes, and in primary, metastatic, and recurrent prostatic adenocarcinoma. Prostate 2003;54:79–87.
12. Zellweger T, Sturm S, Rey S, Zlobec I, Gsponer JR, Rentsch CA, et al. Estrogen receptor beta expression and androgen receptor phosphorylation correlate with a poor clinical outcome in hormone-naive prostate cancer and are elevated in castration-resistant disease. Endocr Relat Cancer 2013;20:403–13.
13. Hershberger PA, Stabile LP, Kanterewicz B, Rothstein ME, Gubish CT, Land S, et al. Estrogen receptor beta (ERbeta) subtype-specific ligands increase transcription, p44/p42 mitogen activated protein kinase (MAPK) activation and growth in human non-small cell lung cancer cells. J Steroid Biochem Mol Biol 2009;116:102–9.
14. Zuguchi M, Miki Y, Onodera Y, Fujishima F, Takeyama D, Okamoto H, et al. Estrogen receptor alpha and beta in esophageal squamous cell carcinoma. Cancer Sci 2012;103:1348–55.
15. Yeh CR, Ou ZY, Xiao GQ, Guancial E, Yeh S. Infiltrating T cells promote renal cell carcinoma (RCC) progression via altering the estrogen receptor beta-DAB2IP signals. Oncotarget 2015;6:44346–59.
16. Sanger HL, Klotz G, Riesner D, Gross HJ, Kleinschmidt AK. Viroids are single-stranded covalently closed circular RNA molecules existing as highly base-paired rod-like structures. Proc Natl Acad Sci U S A 1976;73: 3852–6.
17. Memczak S, Jens M, Elefsinioti A, Torti F, Krueger J, Rybak A, et al. Circular RNAs are a large class of animal RNAs with regulatory potency. Nature 2013;495:333–8.
18. Hansen TB, Jensen TI, Clausen BH, Bramsen JB, Finsen B, Damgaard CK, et al. Natural RNA circles function as efficient microRNA sponges. Nature 2013;495:384–8.
19. Lasda E, Parker R. Circular RNAs: diversity of form and function. RNA 2014;20:1829–42.
20. Hansen TB, Kjems J, Damgaard CK. Circular RNA and miR-7 in cancer. Cancer Res 2013;73:5609–12.
21. Shu X, Hildebrandt MA, Gu J, Tannir NM, Matin SF, Karam JA, et al. MicroRNA profiling in clear cell renal cell carcinoma tissues potentially links tumorigenesis and recurrence with obesity. Br J Cancer 2017; 116:77–84.
22. Song W, Yeh CR, He D, Wang Y, Xie H, Pang ST, et al. Infiltrating neutrophils promote renal cell carcinoma progression via VEGFa/ HIF2alpha and estrogen receptor beta signals. Oncotarget 2015;6: 19290–304.
23. Kramer MC, Liang D, Tatomer DC, Gold B, March ZM, Cherry S, et al. Combinatorial control of Drosophila circular RNA expression by intronic repeats, hnRNPs, and SR proteins. Genes Dev 2015;29:2168–82.
24. Ou Z, Wang Y, Liu L, Li L, Yeh S, Qi L, et al. Tumor microenvironment B cells increase bladder cancer metastasis via modulation of the IL-8/androgen receptor (AR)/MMPs signals. Oncotarget 2015;6:26065–78.
25. Estecha A, Sanchez-Martin L, Puig-Kroger A, Bartolome RA, Teixido J, Samaniego R, et al. Moesin orchestrates cortical polarity of melanoma tumour cells to initiate 3D invasion. J Cell Sci 2009;122:3492–501.
26. Rybak-Wolf A, Stottmeister C, Glazar P, Jens M, Pino N, Giusti S, et al. Circular RNAs in the mammalian brain are highly abundant, conserved, and dynamically expressed. Mol Cell 2015;58:870–85.
27. You X, Vlatkovic I, Babic A, Will T, Epstein I, Tushev G, et al. Neural circular RNAs are derived from synaptic genes and regulated by development and plasticity. Nat Neurosci 2015;18:603–10.
28. Bhan A, Hussain I, Ansari KI, Kasiri S, Bashyal A, Mandal SS. Antisense transcript long noncoding RNA (lncRNA) HOTAIR is transcriptionally induced by estradiol. J Mol Biol 2013;425:3707–22.
29. Llovet JM, Di Bisceglie AM, Bruix J, Kramer BS, Lencioni R, Zhu AX, et al. Design and endpoints of clinical trials in hepatocellular carcinoma. J Natl Cancer Inst 2008;100:698–711.
30. Wijelath ES, Rahman S, Murray J, Patel Y, Savidge G, Sobel M. Fibronectin promotes VEGF-induced CD34 cell differentiation into endothelial cells. J Vasc Surg 2004;39:655–60.
31. Steffens S, Schrader AJ, Vetter G, Eggers H, Blasig H, Becker J, et al. Fibronectin 1 protein expression in clear cell renal cell carcinoma. Oncol Lett 2012;3:787–90.
32. Waalkes S, Atschekzei F, Kramer MW, Hennenlotter J, Vetter G, Becker JU, et al. Fibronectin 1 mRNA expression correlates with advanced disease in renal cancer. BMC Cancer 2010;10:503.

33. Remmele W, Stegner HE. [Recommendation for uniform definition of an immunoreactive score (IRS) for immunohistochemical estrogen receptor detection (ER-ICA) in breast cancer tissue]. Pathologe 1987;8:138–40.
34. Fujimura T, Takahashi S, Urano T, Ogawa S, Ouchi Y, Kitamura T, et al. Differential expression of estrogen receptor beta (ERbeta) and its C-terminal truncated splice variant ERbetacx as prognostic predictors in human prostatic cancer. Biochem Biophys Res Commun 2001;289:692–9.
35. Yu CP, Ho JY, Huang YT, Cha TL, Sun GH, Yu DS, et al. Estrogen inhibits renal cell carcinoma cell progression through estrogen receptor-beta activation. PLoS One 2013;8:e56667.
36. Jeck WR, Sorrentino JA, Wang K, Slevin MK, Burd CE, Liu J, et al. Circular RNAs are abundant, conserved, and associated with ALU repeats. RNA 2013;19:141–57.
37. Xie H, Ren X, Xin S, Lan X, Lu G, Lin Y, et al. Emerging roles of circRNA_001569 targeting miR-145 in the proliferation and invasion of colorectal cancer. Oncotarget 2016;7:26680–91.
38. Li F, Zhang L, Li W, Deng J, Zheng J, An M, et al. Circular RNA ITCH has inhibitory effect on ESCC by suppressing the Wnt/beta-catenin pathway. Oncotarget 2015;6:6001–13.
39. Wang K, Sun Y, Tao W, Fei X, Chang C. Androgen receptor (AR) promotes clear cell renal cell carcinoma (ccRCC) migration and invasion via altering the circHIAT1/miR-195-5p/29a-3p/29c-3p/CDC42 signals. Cancer Lett 2017;394:1–12.
40. Cui ZH, Shen SQ, Chen ZB, Hu C. Growth inhibition of hepatocellular carcinoma tumor endothelial cells by miR-204-3p and underlying mechanism. World J Gastroenterol 2014;20:5493–504.
41. Chen PH, Chang CK, Shih CM, Cheng CH, Lin CW, Lee CC, et al. The miR-204-3p-targeted IGFBP2 pathway is involved in xanthohumol-induced glioma cell apoptotic death. Neuropharmacology 2016;110:362–75.
42. Li JY, Jia S, Zhang WH, Zhang Y, Kang Y, Li PS. Differential distribution of microRNAs in breast cancer grouped by clinicopathological subtypes. Asian Pac J Cancer Prev 2013;14:3197–203.
43. Zaravinos A, Lambrou GI, Mourmouras N, Katafygiotis P, Papagregoriou G, Giannikou K, et al. New miRNA profiles accurately distinguish renal cell carcinomas and upper tract urothelial carcinomas from the normal kidney. PLoS One 2014;9:e91646.
44. Takayasu H, Horie H, Hiyama E, Matsunaga T, Hayashi Y, Watanabe Y, et al. Frequent deletions and mutations of the beta-catenin gene are associated with overexpression of cyclin D1 and fibronectin and poorly differentiated histology in childhood hepatoblastoma. Clin Cancer Res 2001;7:901–8.
45. Qian P, Zuo Z, Wu Z, Meng X, Li G, Zhang W, et al. Pivotal role of reduced let-7g expression in breast cancer invasion and metastasis. Cancer Res 2011;71:6463–74.
46. Tapper J, Kettunen E, El-Rifai W, Seppala M, Andersson LC, Knuutila S. Changes in gene expression during progression of ovarian carcinoma. Cancer Genet Cytogenet 2001;128:1–6.
47. Lou X, Han X, Jin C, Tian W, Yu W, Ding D, et al. SOX2 targets fibronectin 1 to promote cell migration and invasion in ovarian cancer: new molecular leads for therapeutic intervention. OMICS 2013;17:510–8.
48. Yang ZG, Awan FM, Du WW, Zeng Y, Lyu J, Wu, et al. The Circular RNA Interacts with STAT3, increasing its nuclear translocation and wound repair by modulating Dnmt3a and miR-17 Function. Mol Ther 2017; 25:2062–74.
49. Han Y, Liu Y, Zhang H, Wang T, Diao R, Jiang Z, et al. Hsa-miR-125b suppresses bladder cancer development by down-regulating oncogene SIRT7 and oncogenic long noncoding RNA MALAT1. FEBS Lett 2013.
50. Liu XH, Sun M, Nie FQ, Ge YB, Zhang EB, Yin DD, et al. Lnc RNA HOTAIR functions as a competing endogenous RNA to regulate HER2 expression by sponging miR-331-3p in gastric cancer. Mol Cancer 2014;13:92.